

A microfluidic device with integrated optics for microparticle switching

Siew-Kit Hoi, Zhi-Bin Hu, Yuanjun Yan, Chorng-Haur Sow, and Andrew A. Bettiol^{a)}

Department of Physics, National University of Singapore, Blk S12, 2 Science Drive 3, Singapore 117542

(Received 4 July 2010; accepted 16 October 2010; published online 3 November 2010)

We report a high efficiency and noninvasive microfluidic particle switching device with integrated optical microstructures. Microfluidic channels are combined with a cylindrical microlens and an optical fiber to achieve on-chip optical switching of colloidal particles without the need for an optical microscope. A laser beam is coupled into an optical fiber and redirected by the microlens. The angle of incidence of the optical force can be changed by varying the position of the optical fiber relative to the microlens. Under certain circumstances, a switching efficiency approaching 100% was achieved with a relatively fast response time for a solution containing 10 μm polystyrene spheres. © 2010 American Institute of Physics. [doi:10.1063/1.3512902]

Miniaturized fluorescence activated cell sorting (FACS) has been extensively investigated in recent years due to its advantages including infinitesimal sample volume, increased sensitivity, reduced processing time, and device portability.^{1,2} The performance of FACS is determined by the efficiency with which targeted cells can be switched into a desired outlet. Switching schemes based on dielectrophoresis force have been demonstrated as being effective.³ However the electrode fabrication for such devices involves a complex multi-step process that requires high-end fabrication tools and facilities; hindering its implementation for low cost, disposable lab-on-a-chip devices. Optical force may provide an alternative route to a noninvasive, simple, yet effective switching scheme.² Microparticle sorting devices based on optical tweezers rely on a tightly focused laser to attract and change the path of microparticles in a laminar flow environment.^{2,4} In such devices, hydrodynamic focusing is usually necessary in order to ensure that individual particles interact with the tightly focused laser beam. Several other optical switching schemes with improved efficiency that allow for simultaneous manipulation of multiple particles have also been reported.⁵ For example, optical deflection of particles with a reconfigurable near field geometry in a total internal reflection microscope system was employed by Marchington *et al.*⁶ to perform optical sorting within a microfluidic system. An optical line trap was integrated into a microflow channel chip to achieve fluorescence-based activation and sorting by Applegate *et al.*⁷ We have also previously reported a microfluidic device comprised of two crossed microchannels and a line shaped focused laser beam to sort particles in a continuous flow environment.⁸ The major drawback of all the aforementioned optical switching schemes is that their operation relies on the use of an expensive and bulky optical microscope system.

To overcome this limitation, microfluidic systems that integrate optical fibers have been developed.^{9,10} Unlike most of the microscope-based optical switching schemes, optical manipulation with integrated fibers provides additional advantages including simple operation, low cost and portability.¹¹ To date, several schemes that use two well-aligned single-mode fibers have been used to demonstrate the feasibility of particle manipulation by making use of two

counter-propagating laser beams.^{10–12} However, most of the previous fiber based manipulation systems operate under stagnant flow or a very slow flow rate ($<50 \mu\text{m/s}$), which is a drawback when it comes to continuous particle separation.

Here, we present a simple, robust and inexpensive fiber-based compact microfluidic system that is capable of switching and separating particles in a continuous flow environment without the need for a bulky optical microscope. The switching mechanism is based on the propulsion of a microparticle into the desired outlet by light momentum.

The device was fabricated in polydimethylsiloxane using soft lithography from a master mold that was fabricated in SU-8 using the proton beam writing (PBW) technique.¹³ The PBW technique is well suited to fabricating master molds with high aspect ratio and smooth side walls. Figure 1 shows a schematic of the optical fiber-based microfluidic switching system. The physical dimensions of the channels (main channel with width 100 μm , height 35 μm) are shown in the inset of Fig. 1. The device consists of a Y-shaped microchannel with two outlets, collection and waste. The most notable part of the device is the cylindrical microlens that has a radius of curvature of 65 μm . With this integrated lens, we can easily adjust the path of the laser beam that emanates from the optical fiber. The beam direction can be controlled by simply placing the fiber in a different configuration with the aid of a precision alignment stage coupled with guiding grooves. The height of the fluid channels was 35 μm . This height was determined by the diameter of the fiber tips that

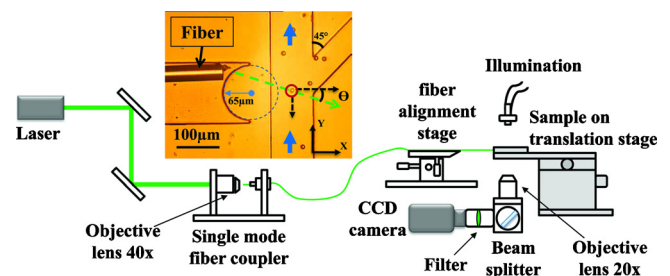


FIG. 1. (Color online) Experimental set up for fiber integrated microfluidic switching system. The inset includes illustration of optical switching with fiber where the cylindrical microlens was used to deflect laser beam for different bias angle θ . The arrow indicates the particle flow direction. The objective lens was used for imaging and optical fiber alignment.

^{a)}Electronic mail: phybaa@nus.edu.sg.

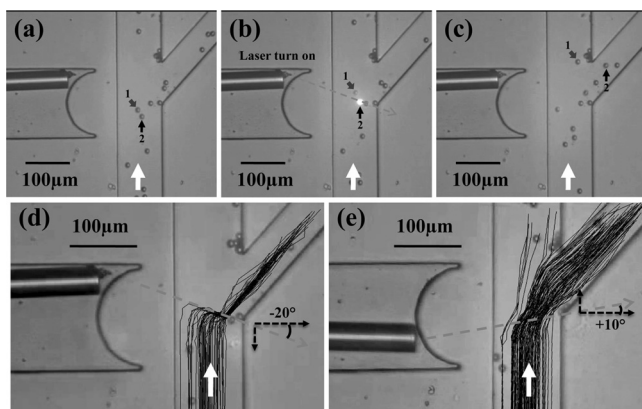


FIG. 2. [(a)–(c)] Consecutive images of PS spheres with a diameter of $10\ \mu\text{m}$ passing through the intersection. (a) Two spheres initially flowing in the channel at $150\ \mu\text{m/s}$. The latter one (2) was targeted to be switched. [(b)–(c)] Laser turned on after the first sphere (1) passed by. The second sphere (2) was propelled into the collection outlet by optical force. The first sphere (1) passed straight through. [(d)–(e)] Trajectories of the particles in two different fiber orientations. Laser (100 mW) beam paths are indicated by the dotted lines. The particles were moving at an average speed of $90\ \mu\text{m/s}$ in both experiments. The white arrows show the direction of fluid flow (enhanced online). [URL: <http://dx.doi.org/10.1063/1.3512902.1>]

were used in the device. The tip of the single-mode fiber (Thorlab, 460HP) was thinned in a one-step chemical etch using hydrofluoric acid for 3 h to a final diameter of $\sim 30\ \mu\text{m}$. A laser (diode pumped solid state laser 532 nm, 250 mW) was coupled into the fiber core with a single-mode fiber coupler (Newport, F-915). The etched tip of the fiber was inserted into the molded vias of width $140\ \mu\text{m}$ using a precision fiber alignment xyz-stage (Newport, 561 UL-TRAlign™). The alignment stage enabled us to vary the fiber configuration and hence introduce a variation in the angle of incidence of the laser. The bias angle (θ , Fig. 1 inset) could be varied from $+20^\circ$ to -20° by placing the fiber tip at different locations within the guide channel. A syringe pump (KD Scientific 250) was used to transport samples continuously through the microfluidic channel. A time resolved imaging system was constructed to capture the full dynamics of the switching events. Still images captured at 25 frames per second were obtained using a charge coupled device camera coupled to a $20\times$ objective lens. The images were subsequently used to determine mean particle velocities.

The operation of the microfluidic optical switching device can be viewed in the video footage provided (see Fig. 2). Particle switching occurs as a result of the interplay between the fluid drag force, optical gradient force and optical scattering force. In order to understand its operation one must consider the forces acting on the microparticles as they move through the channel intersection. The optical gradient

force tends to pull the particle toward the optical axis. The scattering force acting on a particle can be divided into an X and Y component, with the channel wall defining the Y axis (see Fig. 1). The X component of the optical force provides a propelling force to push the particle horizontally. The Y component decelerates or accelerates the particles, depending on the bias angle, θ . Figures 2(a)–2(c) shows consecutive snapshots of the optical switching of PS spheres with a diameter of $10\ \mu\text{m}$ flowing at $150\ \mu\text{m/s}$ in the microchannel. When the laser is turned on, the targeted sphere (2) is pushed to the collection outlet while the first sphere (1) passes straight through. Hence, the two spheres were separated by the optical force.

The trajectories plotted in Figs. 2(d) and 2(e) show how the laser beam bias angle influences the switching efficiency. In both experiments, the laser power was measured to be 100 mW at the fiber tip, and the flow speed of the PS spheres was $90\ \mu\text{m/s}$. When the bias angle was set to -20° [Fig. 2(d)], all the spheres were switched to the collection outlet regardless of their original position. For fiber positions that give a negative bias angle θ , the Y component of the optical force opposes the flow direction and the particles are slowed down. If the stopping force is sufficiently large to overcome the fluid drag force, 100% of the particles can be switched, as shown in Fig. 2(d). When the bias angle is positive, for example $+10^\circ$ as shown in Fig. 2(e), the Y component of the optical force accelerates the particles and the switching efficiency is consequently reduced. Figure 2(e) shows that particles located far from the collection outlet are sometimes not switched.

Figure 3 shows the variation in particle switching percentage as a function of velocity for a bias angle of $\theta = -20^\circ$. The results are taken from a statistical analysis of more than 1000 microspheres. In order to study the effect of the particles' distance from the collection outlet, the particles were grouped according to different zones in the microchannel. As illustrated in Fig. 3(a), the $100\text{-}\mu\text{m}$ -wide channel was equally divided into five zones, labeled 1 to 5. The laser beam path can also be seen in this figure. From the plots of switching percentage for spheres flowing in different zones versus the velocity of the spheres [shown in Fig. 3(b)], it can be seen that all the spheres in zone 4 and 5 were switched into the collection outlet for a constant laser power of 100 mW. For particles that flow in zone 1, 2, and 3, the switching efficiency depends on the velocity of the particles as well as the distance from the outlet. The switching percentage for zone 1 drops drastically as the velocity is increased. In order for the particles in zone 1 to be switched, the Y component of the stopping force must be sufficiently large to overcome the fluid drag force throughout the process of displacing the particle $\sim 80\ \mu\text{m}$ laterally. The interplay between the optical

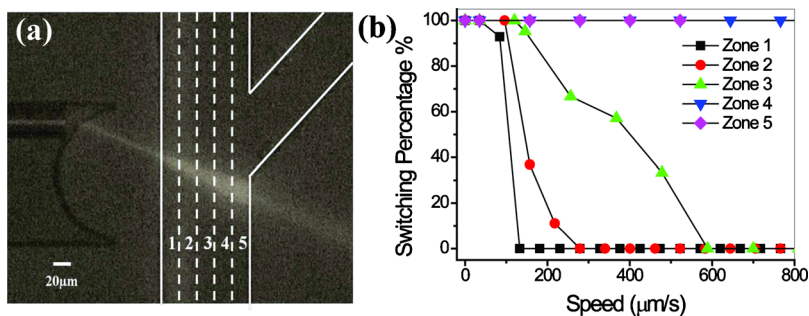


FIG. 3. (Color online) (a) The $100\text{-}\mu\text{m}$ -wide channel was equally divided into five zones, labeled 1 to 5. The figure also depicts the beam path of the laser when the illumination light was turned off. (b) Switching percentage of PS spheres with a diameter of $10\ \mu\text{m}$ vs the velocity of the spheres for different zones. Laser power is 100 mW.

stopping force and the fluid drag force will determine whether a particle is switched. If the velocity of the micro-particle is too high, then for a given laser power there is not enough force to bring it to a stop. The optical stopping force required to overcome the viscous drag force can be estimated by assuming that the two forces balance at the threshold velocity. For zone 1 the threshold velocity is $130 \mu\text{m/s}$. Hence, from the drag force equation, $F_{\text{Drag}} = 6\pi\eta av$, where η is the fluid viscosity, v is the velocity of the sphere with respect to the flowing fluid, and a is radius of the sphere, we deduce that the optical force required to stop the PS spheres with a diameter of $10 \mu\text{m}$ is 12 pN . If we assume that this stopping force is given by $F \sin(20^\circ)$, where F is the net optical force, then the net optical force exerted on the particle is approximately 35 pN .

We also observed that the switching efficiency increases as particles flow closer to the outlet. The maximum velocity of particles that were switched for a constant laser power of 100 mW was $130 \mu\text{m/s}$, $280 \mu\text{m/s}$, and $590 \mu\text{m/s}$ for zone 1, 2, and 3, respectively. This can be attributed to the fact that particles are easier to switch into the collection outlet if the required displacement is shorter. Particles in zone 4 and 5 were observed to go straight only when their speed exceeded $1000 \mu\text{m/s}$ (not shown in Figure). The relatively high velocity that particles can travel and still be switched to a collection channel is an advantage of this method over other switching methods that have been reported.^{10–12}

We have demonstrated a unique microparticle switching device that combines microfluidic channels with on chip integrated micro optical components. Microstructures with optical functionality such as microlenses and optical fibers are built-in to switch particles efficiently by utilizing optical force. It is relatively straight forward to extend this idea to

make a fluorescence activated cell sorting device by including fibers that can measure fluorescence. The measured signals can then be used to modulate the laser power in order to selectively switch microparticles based on their emission properties.

Funding support by the Singapore Ministry of Education (MOE)–Academic Research Fund (AcRF) Tier 2 (Grant No. R-144-000-258-112) is acknowledged.

- ¹A. Y. Fu, C. Spence, A. Scherer, F. H. Arnold, and S. R. Quake, *Nat. Biotechnol.* **17**, 1109 (1999).
- ²M. M. Wang, E. Tu, D. E. Raymond, J. M. Yang, H. C. Zhang, N. Hagen, B. Dees, E. M. Mercer, A. H. Forster, I. Kariv, P. J. Marchand, and W. F. Butler, *Nat. Biotechnol.* **23**, 83 (2005).
- ³L. Wang, L. A. Flanagan, N. L. Jeon, E. Monuki, and A. P. Lee, *Lab Chip* **7**, 1114 (2007).
- ⁴T. D. Perroud, J. N. Kaiser, J. C. Sy, T. W. Lane, C. S. Branda, A. K. Singh, and K. D. Patel, *Anal. Chem.* **80**, 6365 (2008).
- ⁵X.-C. Yuan, S. W. Zhu, J. Bu, Y. Y. Sun, J. Lin, and B. Z. Gao, *Appl. Phys. Lett.* **93**, 263901 (2008).
- ⁶R. F. Marchington, M. Mazilu, S. Kuriakose, V. Garces-Chavez, P. J. Reece, T. F. Krauss, M. Gu, and K. Dholakia, *Opt. Express* **16**, 3712 (2008).
- ⁷R. W. Applegate, J. Squier, T. Vestad, J. Oakey, D. W. M. Marr, P. Bado, M. A. Dugan, and A. A. Said, *Lab Chip* **6**, 422 (2006).
- ⁸S.-K. Hoi, C. Udalgama, C.-H. Sow, F. Watt, and A. A. Bettiol, *Appl. Phys. B: Lasers Opt.* **97**, 859 (2009).
- ⁹R. W. Applegate, J. Squier, T. Vestad, J. Oakey, and D. W. M. Marr, *Appl. Phys. Lett.* **92**, 013904 (2008).
- ¹⁰C. Jensen-McMullin, H. P. Lee, and E. R. Lyons, *Opt. Express* **13**, 2634 (2005).
- ¹¹J. T. Blakely, R. Gordon, and D. Sinton, *Lab Chip* **8**, 1350 (2008).
- ¹²B. Lincoln, S. Schinkinger, K. Travis, F. Wottawah, S. Ebert, F. Sauer, and J. Guck, *Biomed. Microdevices* **9**, 703 (2007).
- ¹³J. A. van Kan, L. P. Wang, P. G. Shao, A. A. Bettiol, and F. Watt, *Nucl. Instrum. Methods Phys. Res. B* **260**, 353 (2007).